

Model for detection of immobilized superparamagnetic nanosphere assay labels using giant magnetoresistive sensors

Mark Tondra^{a)}

Nonvolatile Electronics, Eden Prairie, Minnesota 55344

Marc Porter^{b)} and Robert J. Lipert

Microanalytical Instrumentation Center, Iowa State University, Ames, Iowa 50011

(Received 30 September 1999; accepted 20 March 2000)

Commercially available superparamagnetic nanospheres are commonly used in a wide range of biological applications, particularly in magnetically assisted separations. A new and potentially significant technology involves the use of these particles as labels in magnetoresistive assay applications. In these assays, magnetic bead labels are used like fluorescent labels except that the beads are excited and detected with magnetic fields rather than with photons. A major advantage of this technique is that the means for excitation and detection are easily integrable on a silicon circuit. A preliminary study of this technique demonstrated its basic feasibility, and projected a sensitivity of better than 10^{-12} molar [Baselt *et al.*, *Biosensors Bioelectronic* **13**, 731 (1998)]. In this article we examine the theoretical signal to noise ratio of this type of assay for the special case of a single magnetic bead being detected by a single giant magnetoresistive (GMR) detector. Assuming experimentally observed and reasonable parameters for the magnetic label and the sensitivity of the GMR detector, the signal to noise ratio is calculated to be greater than 5000:1 for detection of a single $1\ \mu\text{m}$ diameter magnetic microsphere immobilized on the surface of a $1\ \mu\text{m} \times 1\ \mu\text{m}$ GMR sensor. Based on this large signal to noise ratio, the detection format should be applicable to more complicated assays where linear quantification is required or to assays requiring significantly smaller beads. Detection of microsphere labels approaching 10 nm may be possible upon further technological advances. © 2000 American Vacuum Society. [S0734-2101(00)11804-4]

I. INTRODUCTION

Magnetic particles have been used for many years in biological assays.^{1,2} These particles range in size from a few nanometers up to a few microns, and in composition from pure ferrite to small percentages of ferrite encapsulated in plastic or ceramic spheres. The beads are subsequently coated with a chemical or biological species that selectively binds to the target analyte.³⁻⁶ To date, these types of particles have been used primarily to separate and concentrate analytes for off-line detection.⁵⁻⁸

These particles can be part of a completely magnetic quantitative assay with the use of a magnetic detector. Two examples of magnetic assay detectors are using an ac magnetic susceptibility technique⁹ and a superconducting quantum interference device (SQUID) magnetometer¹⁰ to quantify the magnetic signal from analyte solutions. In this article we discuss the use of integrated giant magnetoresistive (GMR) sensors as the magnetic detectors in these applications. GMR sensors have the unique advantage of being compatible with silicon integrated circuit fabrication technology, resulting in a detector that can be made on a single chip along with any of the needed electrical circuitry. Results from theoretical modeling are presented showing magnetoresistive detectors have single-bead resolution for micron sized beads. The results also suggest that, since the lower limit on bead size detection is set by the lithographical feature size,

detection of single 100 nm beads is possible with existing technology, and may reach 10 nm in the near future.

This kind of sensitivity to extremely small magnetic objects is already convincingly demonstrated in the ubiquitous hard disk drive-read head system present within every personal computer. State-of-the-art read heads can detect a $20\ \text{nm} \times 500\ \text{nm}$ bit on a magnetized surface with great reliability and at extremely high speed.¹¹ Billions of these on-chip detectors are fabricated each year in the form of hard disk drive read heads at a cost of $\sim \$1$ per head. The required sensitivity of these detectors is achieved by making the GMR sensor as small as the objects being detected, and by getting the sensor very close ($< 100\ \text{nm}$) to the surface of the hard disk.

Analogous steps must be taken in the GMR bead assay. Recently, such a system was reported where bare (unpacked) GMR sensors were used, permitting the beads to come within $\sim 1\ \mu\text{m}$ of the GMR detector and were able to detect single $2.8\ \mu\text{m}$ Dynal M280 beads.¹² The authors measured the sensitivity of the GMR detector to magnetically labeled analytes, and calculated a minimum detectable concentration of analyte to 65 000 molecules/ml when mass transport limitations are accounted for. The system was expanded and currently is capable of detecting 64 different analytes on the same chip.¹³ In this article we consider in detail the ideal case of a single immobilized $1\ \mu\text{m}$ bead being detected by a $1\ \mu\text{m} \times 1\ \mu\text{m}$ GMR detector. It is shown, using reasonable parameters for bead properties and GMR characteristics, that the signal to noise ratio of this model system is greater than

^{a)}Electronic mail: markt@nve.com

^{b)}Electronic mail: mporter@porter1.ameslab.gov

5000:1. This high signal to noise ratio suggests that the GMR assay can be adapted to a great many applications.

II. OVERVIEW OF DETECTION FORMAT

The magnetoresistive bead detection format requires the immobilization of a magnetically labeled analyte in close proximity to an integrated GMR. Because the focus of this article is on the detection of the label, and not its immobilization, details of binding techniques will not be discussed. It is assumed that the immobilization is sufficient to hold the label close to the GMR in the presence of moderate (< 20 mT) magnetic fields, and that the immobilization means does not add significantly to the distance from the bead to the GMR detector. The proximity of the bead to the GMR detector is critical because the fields from these beads are very localized, roughly decaying as $1/r^3$, where r is the distance from the center of a bead and the GMR surface. This field distribution will be calculated in Sec. IV.

Once a bead is immobilized, it must be magnetized by applying an external magnetic field. This is because commercially available paramagnetic beads have minimal and ill-defined remnant magnetization (i.e., the magnetization remaining after an external magnetizing field is removed). The field from a bead that is detected by a GMR is proportional to the magnetization of the bead, which is in turn proportional to the applied field. The GMR detector also responds to the component of excitation fields along its sensitive axis, and will magnetically saturate at some point. A critical issue, then, is to be able to apply sufficient fields to magnetize the beads without saturating the detector.

Beads for assay purposes can be obtained from several commercial sources. Sizes range from 30 nm to $5 \mu\text{m}$. The larger particles typically have small amounts of ferromagnetic material dispersed in a plastic or ceramic matrix. The actual function of the assay is controlled by the specific coating on the surface of the bead. Applications range from bacterial concentration to immunoassays.⁵⁻¹⁰ These coatings are generally nonmagnetic, and do not affect detection other than to increase the separation between a bead and the GMR. Before a more detailed analysis of the bead detection magnetics, the fabrication of GMR detectors is described.

III. SENSOR FABRICATION

A GMR detector consists of a stack of thin, alternating magnetic and nonmagnetic metallic layers. The resistivity of this material is a function of the external magnetic field.¹⁴⁻¹⁶ The resistivity varies with the angle (θ) between the magnetizations of adjacent magnetic layers with a $\sin \theta$ dependence. A typical change in resistivity from minimum (when the magnetizations of magnetic layers are aligned in parallel) to maximum (when magnetizations are aligned antiparallel) is $\sim 15\%$ of the minimum value. These thin film stacks are fashioned into resistive sensors by patterning the material into long stripes. The observed resistance is then proportional to the length and inversely proportional to the width of a stripe. A typical sheet resistance is $10 \Omega/\square$. Consequently, a GMR resistor with a respective width and length of 0.5 and

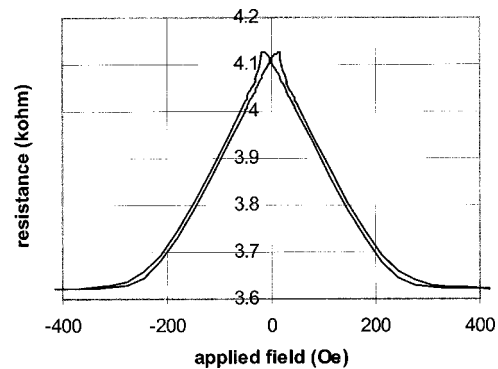


FIG. 1. Response of a NVE multilayer GMR to an applied field. Note that the best area for operating in a linear mode is at ± 100 Oe (10 mT). The exact composition of the multilayer is $\{[\text{NiFeCo}_3/\text{CoFe}_{1.5}/\text{CuAgAu}_{1.5}/\text{CoFe}_{1.5}]_4/\text{NiFeCo}_3\}$ (all thicknesses in nm).

$5.0 \mu\text{m}$ ($10 \square$) would have a resistance of 100Ω under parallel magnetization that increases to 115Ω (15%) under antiparallel magnetization. When correctly designed, the response of a GMR resistor to an external magnetic field is unipolar and linear. The saturation field is controllable over a range from 1 to a few tens of mT, depending upon the magnetic design. The observed resistance versus field strength of a such a linear resistor, patterned from Nonvolatile Electronic's (NVE's) "standard multilayer" material, is plotted in Fig. 1.

GMR films are typically deposited on insulating or semiconductor substrates in vacuum deposition systems by dc-magnetron, rf diode, or ion beam sputtering. The stack thickness is tens of nanometers, with individual layers within the stack controlled to tenths of nanometers. Patterning of the films follows typical photolithographic techniques and acid/ion milling etching processes.

These general techniques are directly applicable to the magnetoresistive bead assay application. The key to successful design is to adjust the GMR detector size so that all of the magnetoresistive material is as close as possible to the beads being detected. This implies both a reduction in the lateral dimensions (length and width) of the detector, and minimization of the distance between the bead and detector. The schematic in Fig. 2 suggests such a design.

IV. DETECTION MAGNETICS

We now demonstrate, by theoretical consideration, that the fields from a single commercial magnetic bead can be detected by an integrated GMR. For this discussion, we define the Cartesian coordinates for bead detection in the following way: the bead is at the origin, and the GMR detector is parallel to the X - Y plane but at a distance

$$z = a + \nu \quad (1)$$

from the bead's center, where a is the bead radius and ν is the vertical separation from the bead surface to the GMR detector. Further, assume the GMR detector is a $1 \mu\text{m} \times 1 \mu\text{m}$ square whose center is directly beneath the bead at

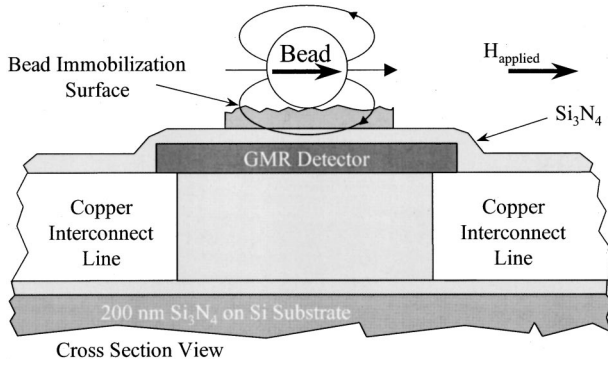


FIG. 2. GMR sensor optimized for minimum separation from the bead to the GMR material. The Si_3N_4 passivation can be as thin as 10 nm. The bead immobilization surface can be 10 nm thick or so. Its precise composition is tuned to the assay being performed. The interconnection lines are buried underneath the GMR element in a further effort to allow the bead and GMR to be as close as possible.

$[0, 0, -z]$ and has edges at $[+/- 0.5, 0, -z]$ and $[0, +/- 0.5, -z]$. The GMR detector is only sensitive along one axis in the plane of the film, which is set to be the X direction. This situation is shown in Fig. 3.

Detection takes place by applying a uniform external magnetic field \mathbf{H}_{app} along the X axis and measuring the stray fields from the bead's induced magnetization, \mathbf{M} . Stray fields from the bead, referred to as \mathbf{H}_{bead} , are not at all uniform, but have their largest magnitude in the X direction. The GMR detector resistance changes linearly in response to the X component of \mathbf{H}_{bead} . Consequently, the X component of \mathbf{H}_{bead} must be calculated over the surface of the GMR detector.

Using SI units, the basic equations relating magnetic induction \mathbf{B} (Wb/m^2), magnetic field strength \mathbf{H} (A/m), and magnetization \mathbf{M} (A/m) are

$$\mathbf{B} = \mu_0(\mathbf{H} + \mathbf{M}), \quad (2)$$

$$\mathbf{M} = \chi_m \mathbf{H}_{\text{app}}, \quad (3)$$

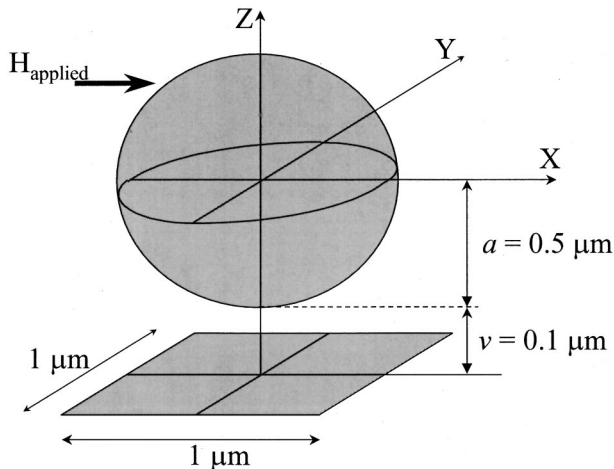


FIG. 3. Coordinate system used for the present calculations. The detector's sensitive axis is the X axis.

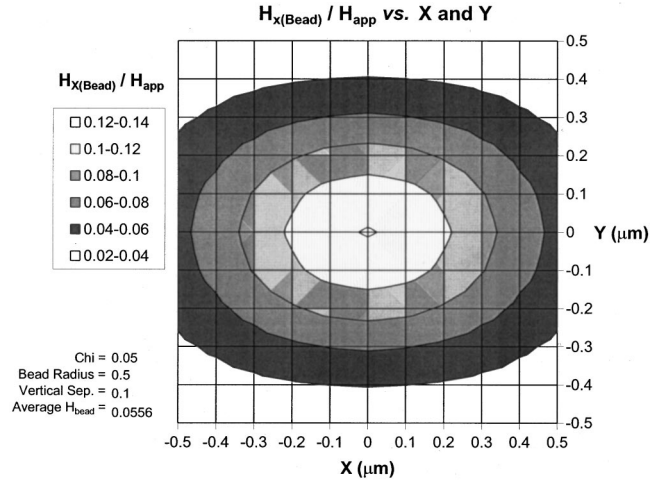


FIG. 4. X -axis field beneath a magnetized bead. The X and Y axes represent the distance (in μm) from the point directly beneath the center of the bead, which is situated above the surface of the GMR in the Z direction by a distance equal to the bead radius plus the vertical separation. The Y -axis field from the bead in the GMR plane is negligibly small. The Z -axis field is sizable, but the GMR detector is not sensitive to fields along the Z axis.

where χ_m is the dimensionless magnetic susceptibility. A spherical bead of superparamagnetic or ferromagnetic material will be uniformly magnetized in a uniform field. The external field from the magnetized bead will have a dipole distribution from an effective dipole moment \mathbf{p} :

$$\mathbf{p} = \mathbf{M}(4\pi/3)a^3, \quad (4)$$

where a is the bead radius, and \mathbf{M} (A/m) is the magnetization.

The two components of the dipole field at location \mathbf{r} from the center of a bead are

$$\mathbf{H}_r = \chi_m \mathbf{H}_{\text{app}} (8\pi/3)(a^3/|\mathbf{r}|^3) \cos(\theta), \quad (5)$$

and

$$\mathbf{H}_\theta = \chi_m \mathbf{H}_{\text{app}} (4\pi/3)(a^3/|\mathbf{r}|^3) \sin(\theta), \quad (6)$$

where θ is the angle between \mathbf{r} and \mathbf{M} (\mathbf{M} is parallel to \mathbf{H}_{app}).

The direction of \mathbf{H}_{bead} from a bead in a uniform applied field in the plane of the page from left to right is roughly depicted in Fig. 2. Note that the field directly under the bead (at $\theta = \pi/2$) due to its magnetization *directly opposes the applied field*. Setting $\chi_m = 0.05$, $a = 0.5 \mu\text{m}$, and $v = 0.1 \mu\text{m}$, the X component of \mathbf{H}_{bead} can be calculated as a function of X and Y . The results of this calculation are shown in Fig. 4. Note that the fields plotted in Fig. 4 are in the opposite direction from the applied field. The total field on the GMR detector is the sum of \mathbf{H}_{app} and \mathbf{H}_{bead} . Since \mathbf{H}_{bead} is always opposite to but smaller than \mathbf{H}_{app} , the net field will never be greater than \mathbf{H}_{app} , or less than zero. The average effect in the example given is $\mathbf{H}_{\text{bead}} = 0.05\mathbf{H}_{\text{app}}$, so the net field is $\mathbf{H}_{\text{total}} = 0.95\mathbf{H}_{\text{app}}$.

Clearly, the effect is limited to the region immediately beneath the bead. The magnitude of the field distortion due to the bead drops off approximately as $1/|\mathbf{r}|^3$ as one moves away from the bead in all directions. Consequently, for

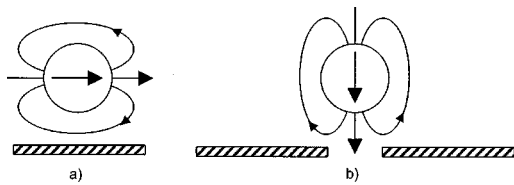


FIG. 5. GMR resistors represented by the thin, hashed rectangles. Both (a) and (b) are cross sections analogous to that in Fig. 2. (a) Resultant bead magnetization and stray fields from an excitation field in the plane of the GMR. (b) Resultant magnetization and fields from a vertical excitation field. In both cases, the GMR resistors respond to the fields in the plane of the GMR film.

single bead detection, it is best to match the GMR detector size to the bead size for maximum resolution.

There are several variations of this technique involving the relative orientation of the beads, GMR detectors, and excitation fields. An important variation of the excitation field geometry is to apply a field normal to the plane of the GMR sensor (see Fig. 5). The GMR is about 1000 times harder to magnetize in the normal direction, so a much larger magnetizing field can be applied to the beads without saturating the GMR sensors. Another important variation from an instrumentation standpoint is having a differential sensor or bridge sensor setup where one or two of several GMR resistors are exposed to fields from the beads while the rest are not, or are exposed to fields in the opposite direction. Additional features could include embedded field excitation straps (extra “wires” can be included in the design of the detectors, which apply a local field of about 0.1 mT/mA) and thick magnetically permeable “flux pipes” that guide magnetic flux around the detector surface much like yokes and cores for electromagnets.

V. DETECTOR SIGNAL TO NOISE

The foregoing model assumes a $1\ \mu\text{m} \times 1\ \mu\text{m}$ GMR detector sits directly beneath the paramagnetic label. Such a detector would carry 5 mA, and have a 10–11 Ω resistance corresponding to \mathbf{H}_{app} ranging from 20 to 0 mT. This represents the 10% resistance change over 20 mT indicated in Fig. 1. The detector voltage, then, changes at a rate of $250\ \mu\text{V}/\text{mT}$. The maximum \mathbf{H}_{app} possible without saturating the sensor is 20 mT. The field attenuation from the bead modeled above is, on average, 0.05 times the \mathbf{H}_{app} . Although the total resistance change will be slightly less than the average field change due to current redistribution within the GMR sensor, assume for now that the net resistance change is exactly proportional to the average field change. Hence, the maximum total signal field is 1.0 mT ($0.05 \times 20\ \text{mT}$). The voltage “signal” from the bead is then $250\ \mu\text{V}$.

The noise of the detector has two main components: the Johnson noise and current dependent $1/f$ noise. The Johnson (thermal) noise for a 10 Ω resistor is $0.4\ \text{nV}/\sqrt{\text{Hz}}$. The detector’s intrinsic $1/f$ noise will typically be two orders of magnitude higher than the thermal noise at 1 Hz, and have a corner frequency at 10 kHz. Assuming a 1 Hz measurement frequency, the total noise will be dominated by the $1/f$ noise,

and be about $40\ \text{nV}/\sqrt{\text{Hz}}$. So the signal to noise ratio at 1 Hz with a 1 Hz bandwidth is $250\ \mu\text{V}/40\ \text{nV} = 6250:1$. While this simple calculation ignores engineering challenges that must be addressed to fully use the available signal, it is clear that detection of a single $1\ \mu\text{m}$ diameter bead with a $1\ \mu\text{m} \times 1\ \mu\text{m}$ GMR detector is not limited by fundamental signal to noise issues.

VI. ULTIMATE SIZE LIMITS AND CONCLUSION

The preceding discussion shows that a GMR sensor can detect a single paramagnetic bead of **any size** as long as the following conditions are met: (1) the sensor is about the same size as the bead, (2) the bead surface is about 0.2 bead radii away from the surface of the sensor, (3) the bead has a χ_m of 0.05, and (4) the GMR sensor response is adequate. All four of these conditions are presently easily met at a bead radius, a , of 500 nm. Reducing a to 100 nm is clearly possible by overcoming technical difficulties in fabrication of the GMR sensors. A significant difficulty will be fabricating increasingly thin passivation layers over the GMR sensor that can withstand the chemical treatment and saline environment required in an assay. Reducing a further to 10 nm will require advances in bead fabrication technology as well as GMR sensor fabrication. Getting a to 1 nm will require new understanding of the fundamental magnetism of extremely small objects. Most of these advances in nanoscale magnetic technology will likely be driven by the hard disk drive industry as they continually decrease bit sizes at a rate of over 60%/year. Advances in magnetic density will complement other rapidly decreasing feature sizes for integrated devices. Ultimately, it may be possible to make these detectors to have the same volume as the objects they are designed to detect.

This design study has described in detail the design for constructing a single bead detector for a magnetoresistive assay. Furthermore, the signal to noise of such an assay was shown to be greater than 5000:1 using reasonable assumptions about the GMR detector and bead properties. In some preliminary experiments, nonoptimized GMR detectors have been used to detect single magnetic beads with signal to noise of several hundred. The most difficult aspect of these experiments has been the precise positioning of the beads with respect to the GMR sensor. Further work is being done to more completely verify the detection limits of this assay format.

ACKNOWLEDGMENTS

The authors thank Art Pohm and John Anderson of NVE, and Jing Ni, Brent Dawson, Mike Granger, and Ruth Shinar of the MIC at Iowa State University for helpful discussions about the GMR bead assay.

¹*Scientific and Clinical Applications of Magnetic Carriers*, edited by U. Hafeli, W. Schutt, J. Teller, and M. Zborowski (Plenum, New York, 1997).

²I. Safarik and M. Safarikova, in Ref. 1, p. 323.

³R. V. Mehta, R. V. Upadhyay, S. W. Charles, and C. N. Ramchand, *Biotechnol. Tech.* **11**, 493 (1997).

- ⁴G. T. Hermanson, *Bioconjugate Techniques* (Academic, New York, 1996).
- ⁵R. S. Molday and D. Mackenzie, *J. Immunol. Methods* **52**, 353 (1982).
- ⁶H. P. Khng, D. Cunliffe, S. Davies, N. A. Turner, and E. N. Vulfson, *Biotechnol. Bioeng.* **60**, 419 (1998).
- ⁷M. Zborowski, C. B. Fuh, R. Green, L. Sun, and J. J. Chalmers, *Anal. Chem.* **67**, 3702 (1995).
- ⁸M. Zborowski, C. B. Fuh, R. Green, N. J. Baldwin, S. Reddy, T. Douglas, S. Mann, and J. J. Chalmers, *Cytometry* **24**, 251 (1996).
- ⁹C. B. Kriz, K. Radevik, and D. Kriz, *Anal. Chem.* **68**, 1966 (1996).
- ¹⁰R. Kötitz, H. Matz, L. Trahms, H. Koch, W. Weitschies, T. Rheinländer, W. Semmler, and T. Bunte, *IEEE Trans. Appl. Supercond.* **7**, 3678 (1997).
- ¹¹H. C. Tong *et al.*, INTERMAG, Kyongju, Korea, 1999.
- ¹²D. R. Baselt, G. U. Lee, M. Natesan, S. W. Metzger, P. E. Sheehan, and R. J. Colton, *Biosens. Bioelectron.* **13**, 731 (1998).
- ¹³R. L. Edelstein, C. R. Tamanaha, P. E. Sheehan, M. M. Miller, D. R. Baselt, L. J. Whitman, and R. J. Colton, *Biosens. Bioelectron.* **14**, 805 (2000).
- ¹⁴G. A. Prinz, *Phys. Today* **48**, 58 (1995).
- ¹⁵J. M. Daughton, P. Bade, M. Jenson, and M. Rahmati, *IEEE Trans. Magn.* **28**, 162 (1992).
- ¹⁶J. M. Daughton, *IEEE Trans. Magn.* **30**, 364 (1994).